Available online at www.sciencedirect.com
SCIENCE DIRECT®

Journal of the European Ceramic Society 24 (2004) 2825–2833
www.elsevier.com/locate/jeurceramsoc

Processing and properties of a glass-ceramic from coal fly ash from a thermal power plant through an economic process

Jae Myung Kim, Hyung Sun Kim*

Department of Materials Science and Metallurgical Engineering, Sunchon National University, Sunchon, 540-742, South Korea

Received 10 April 2003; received in revised form 15 August 2003; accepted 21 August 2003

Abstract

Coal fly ash from a thermal power plant with the addition of selected oxides was used for the preparation of a glass-ceramic with high mechanical properties through an economic process. The starting materials were fly ash, shell (ark shell) as a source of CaO and TiO_2 as a nucleating agent to reduce the melting temperature and to promote internal crystallization. A nuclei formed with Fe and Ti ions from the ash components and added materials, respectively, which had a synergetic effect to induce nuclei in the glass for devitrification. Under a single stage heat treatment, a new crystalline phase formed in the microstructure of glass-ceramics having a crystal size of $2.09\times0.36\times0.096$ μm^3 with a high aspect ratio, 12. The resulting mechanical properties (hardness, strength, fracture toughness, elastic constant and wear rate) of the glass-ceramic indicated good possibilities for use in structural materials.

Keywords: Coal ash; Fly ash; Glass-Ceramics; Mechanical properties; Microstructure-final; Waste materials

1. Introduction

For the recycling and exploitation of coal fly ash, several approaches have been taken over half a decade to develop a glass-ceramic from coal fly ash produced by power plants.[1,2] Typically, glass-ceramics obtained from fly ash have been produced by a combination of melting the fly ash and a one or two stage heat treatment for crystallization, nucleation and crystal growth.[3–8] Other approaches involving a sintering process have also been used.[9]

The properties of glass-ceramics differ according to the makeup of components and the heat treatment conditions. In general the major component found in the ash is CAS ($CaO–Al_2O_3–SiO_2$), with minor components such as MgO, Fe_2O_3 present in order to form crystalline phases. In order to devitrify fly-ash glass after melting, the composition of the ash is modified in terms of composition for internal crystallization. There are several ways to modify the composition of the fly ash: (1) by adding TiO_2 to the coal fly ash as a crystallization catalyst,[10] (2) the addition of inorganic wastes such as SiO_2, CaO, and Na_2O as a glass cullet, and CaO, and MgO as a float dolomite to promote the formation of amorphous and semicrystallized materials,[8] (3) to produce a glass by adding Na_2O (10 wt.%) and melting at 1200 °C,[11] (4) adding CaO (10 wt.%) and Na_2O (10 wt.%) as fluxing additives (however, the melting temperature of 1520 °C for 2 h was found to be too high),[5] and (5) melting at 1550 °C for 3 h without the addition of any other components.[12] The various processes for the production of glass-ceramics using fly ash from power plants are listed in Table 1. The main composition and heat treatment conditions do not differ greatly, however there are a variety of types of crystalline phases in the final product according to the presence of any of the minor components.

For this reason, a modification of the casting process is proposed, whereby the glass-ceramic is examined in terms of its composition and the conditions under which it was processed. Our approach to the development of a glass-ceramic using an economical process was to design the composition of the ash with shell as the raw material. As raw materials, TiO_2 and CaO (using ark shell as the source of the CaO) were selected as nucleating agents and also to decrease the melting temperature of

* Corresponding author. Tel.: +82-61-750-3555; fax: +82-61-750-3550.
E-mail address: hskim@sunchon.ac.kr (H.S. Kim).

0955-2219/$ - see front matter © 2003 Elsevier Ltd. All rights reserved.
doi:10.1016/j.jeurceramsoc.2003.08.012

Table 1
Summary of various possible processes for glass-ceramics derived from power plant fly ashes

Raw materials			Processes		Products	References
Fly ashes		Adding materials	Temperature (°C)	Time (h)	Crystalline phase	
Major components	Minor components					
CAS	MgO	Fe_2O_3	800, 1000	2 2	diopside, anorthite, bustamite, wollastonite,	4
CAS	Fe_2O_3	Na_2O, CaO	800,	2	esseneite, nepheline	5
CAS	Fe_2O_3	MgO	1000	8	albite, anorthite, augite, diopside, wollastonite	6
CAS	Fe_2O_3	MgO, TiO_2	730, 900	8, 20	anorthite, cordierite	7
CAS	Fe_2O_3	MgO	1100	2	feldspar, pyroxene	8

CAS:CaO, Al_2O_3, SiO_2.

the fly ash, meaning a more economical process. This also produced a glass ceramic with good mechanical properties. The present work focuses on the control of the microstructure, producing a high aspect ratio of crystals in order to improve the fracture toughness of the glass-ceramic.

2. Experimental

The glasses for this study were prepared by melting 60 g of ash with the oxides CaO (10, 20, 30 wt.%) (using ark shell as a source of CaO, (CaO:98.93; Na_2O:1.07 wt.%) and TiO_2 (2,5,7,11 wt.%) in Pt-Rh crucibles at 1400 °C for 3 h. The melts were poured into a carbon mold and annealed at $T_g + 10$ °C. Glass transition (T_g) and crystallization temperatures (T_p) were examined by DTA (DTA-TA 1600, USA) using glass powders (212–425 μm, <38 μm) at a heating rate of 10 °C/min.

The thermal expansion coefficients of the glass and glass-ceramic were measured with a dilatometer (Dilatronic, Theta Industrial Inc., USA) in the temperature range of rt—350 °C at a heating rate of 5 °C/min. For SEM (scanning electron microscope; Japan, Hitachi Co., S-3500N) and FESEM (field emission scanning electron microscope; Japan, Hitachi Co., S-4200) observation, the samples were polished and then etched with 2%HF for 10 s. To identify the nuclei composition, EDS (energy dispersive X-ray spectroscopy, Oxford Instrument, AN1000) was used for the glass-ceramic. The crystalline phase was identified by powder X-ray diffraction (XRD, X'Pert APD system, Philips, Netherlands), and the Miller indices and lattice parameters of the new crystal were determined by means of UNITCELL and XRD2000 software (SoftDisc, Korea) respectively, using Cu$K\alpha$ radiation. The crystal growth rates were determined by measuring the surface crystal growth thickness as a function of temperature using an optical microscope (Japan, Olympus Co., BH2-UMA). The aspect ratio of the crystal was measured by an image analyzer from SEM photos.

Density was determined by the Archimedes method and hardness by a micro Vickers indenter (Vickers hardness tester, MVK-E3, Akasi, Japan). Fracture toughness was measured by indentation method and was calculated using the equation proposed by Antis et al.[13] Flexural strength was determined by four-point loading test bars of 3 mm×3 mm×30 mm length at a cross head speed of 0.5 mm/min. Elastic constant of specimens were determined by ultrasonic pulse echo (Panametrics 5800, USA). Erosion was measured as the mass lost from the sample target per mass of SiC impacting particle (size 75 μm, impacting angle 45°).

3. Results and discussion

3.1. Preparation of glass and crystallization

As shown in Fig. 1, a weight reduction of 12% in the range of 440–810 °C means that unburned carbon in

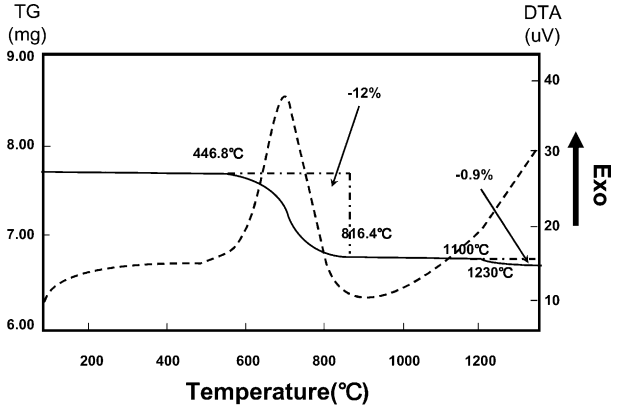

Fig. 1. TG-DTA data of fly ash (as received).

the fly ash is dissociated thermally. On the other hand, an exothermal reaction started at 500 °C and showed the peak reaction at around 700 °C to accompany a carbon oxidation.

The effect of the addition of TiO_2 and CaO to the fly ash on the melting temperature and crystallization temperature is presented in Fig. 2. The increase of CaO in the fly ash showed a noticeable effect in reducing the melting temperature, due to the CaO decreasing the ratio of network formation oxides to breaker oxides, meaning the viscosity of glass became lower. But the effect of TiO_2 in the T_p of glasses was more limited in the range, less than 5 wt.% of TiO_2. On the other hand, the addition of CaO and TiO_2 did not suggest any dependence on T_p due to the glass powder size (a fine powder). In the content of TiO_2, above 5 wt.%, the ΔT_p was small and kept a constant value according to the amount of TiO_2 content for all samples (10–30 wt.% of CaO) as shown in Fig. 3. However, we were unable to find a similarly consistent effect on the ΔT_p when the content of CaO was altered. Thus using the ΔT_p technique for understanding the crystallization mechanism of glass-ceramics,[14] above 5 wt.% of TiO_2, it was shown that the crystallization was based on the internal type rather than the surface type.

As shown in Fig. 4, the crystallization of glass results from internal crystallization because (1) there are no exothermal reaction peaks in the DTA curve for the bulk glass sample not containing TiO_2 (Fig. 4c), and (2) there is no difference in the exothermal peak temperature in Fig. 4a and b for fine and coarse glass powder (different surface area of glass) with 5 wt.% of TiO_2.

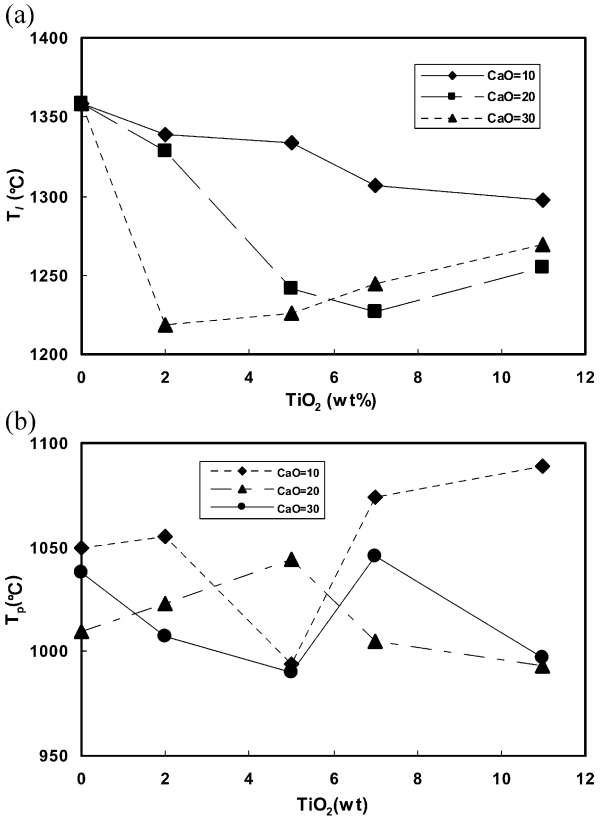

Fig. 2. (a) Liquidus (T_l) and (b) exothermal peak (T_p) temperature of glass (coarse powder, 212–425 μm) determined by DTA analysis as a function of TiO_2 and CaO content (in wt.%).

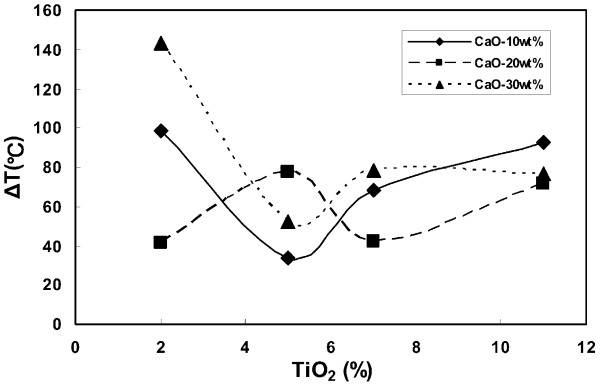

Fig 3. Effect of TiO_2 content on the ΔT_p, the difference of two exothermal peak temperature for different glass powder size (DTA sample), coarse (212–425 μm) and fine powder glass (<38 μm).

3.2. Microstructure of glass-ceramics

The surface crystal morphology of samples not containing TiO_2 and the surface crystal rate as a function of heat treatment temperature are represented in Fig. 5. The rapid growth at 1100 °C is related to the lower viscosity of glass close to the liquidus temperature (1350 °C). The composition of the surface crystals was found to be $Al_2O_3{\cdot}1.11CaO{\cdot}2.93SiO_2$ by EDS, which is similar to the albite phase [$Na(AlSi_3O_8)$](JDPDS, 71-1156). This phase was confirmed with the XRD peak (Fig. 6). Based on the result of thermal analysis, fly ash with TiO_2 and CaO was heated to 1450 °C and held for 3 h, then cooled to 950–1050 °C to enable glass

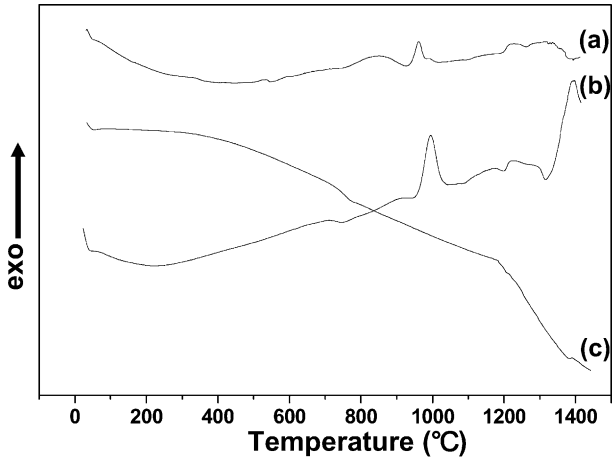

Fig. 4. DTA traces of (a) fine (<38 μm) and (b) coarse glass powder (212–425 μm) 10 wt.% CaO–5 wt.% TiO_2 and (c) bulk glass with only 10 wt.% CaO (without TiO_2).

crystallization, and finally cooled to room temperature in a furnace. Fig. 7 shows the microstructure of glass-ceramics produced under a one stage heat treatment, including the sequence of crystal growth over time at 950 °C. Based on the result of heat treatment at 950 °C, three stages were classified in terms of the nucleation and crystal growth process: (1) nucleation stage for 5–15 min (2) active crystal growth stage for 20–60 min and (3) a steady stage of crystal growth and no change of crystal size for 120–240 min. Thus, the observation of crystal morphology suggests a combined mode, nucleation and crystal growth according to the Tammann curve,[15] (which was not investigated in this study) and gives a positive result for a one-stage heat treatment rather than two stages (nucleation and crystal growth).

Glass which was non-isothermally heat-treated at 880 °C showed an extremely small droplet size (nuclei-like) microstructure just before the exothermal reaction based on Fig. 4, as shown in Fig. 8. The sphere was found to be an amorphous phase rather than crystalline

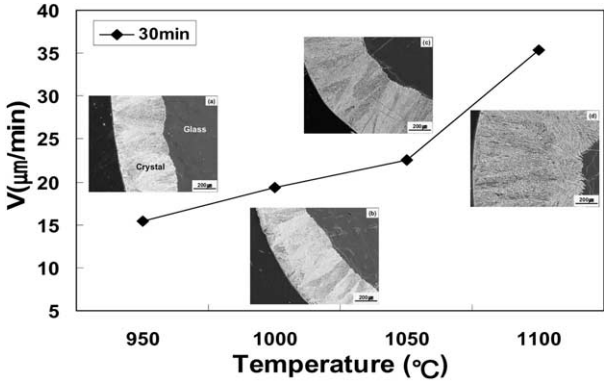

Fig. 5. Surface crystal morphology and surface crystal growth rate of glasses (CaO30 wt.%) heat treated at (a) 950, (b) 1000, (c) 1050 and (d) 1100 °C for 30 min.

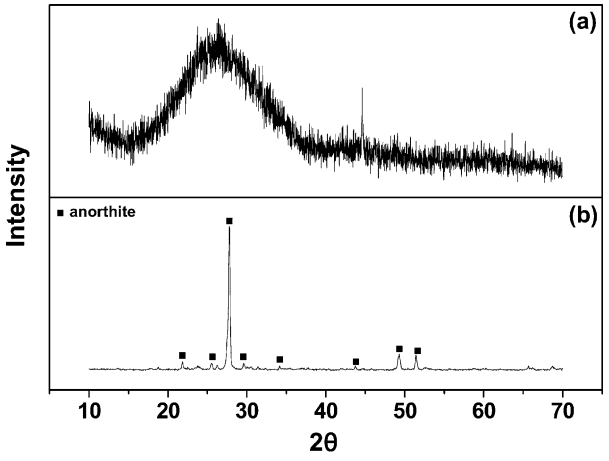

Fig. 6. XRD results of (a) glass and (b) surface crystal (at 1000 °C for 120 min) [in Fig. 6(a) a peak at 45° is resulted from the effect of a sample holder].

structure, suggesting that phase separation is involved in the process. The droplet had a relatively high content of Fe and Ti compared with the residual glass region (Table 2).

The nucleation rate-like curve obtained from DTA is presented in Fig. 9. The maximum nucleation rate in the glass was supposed to be at approximately 770 °C, which is $T_g(700)+70$ °C. However the glass was devitrified through a single stage heat treatment, during a non-isothermal process. The fly ash was heated to the melting temperature of 1450 °C and held for 3 h, and then the molten glass was poured into a graphite mold pre-heated to 750 °C. After casting in the mold, the glass sample was moved into a furnace for crystallization at 950–1050 °C for 10–240 min and was then cooled to room temperature in the furnace. The crystallization was a result of nucleation and crystal growth simultaneously from the simple cycle heating process.

This study found that the effect of temperature on the crystal growth is more noticeable than that of time. In Fig. 10, the microstructure is denser and composed of small-sized crystals ($1.4\times0.11\times0.1$ μm^3) below 1000 °C, but above 1000 °C the crystal size increases ($2.09\times0.36\times0.096$ μm^3) and the orientation of the crystalline phase becomes scattered. With increasing temperature and time, the aspect ratio of the crystal increased, but this was reversed at temperatures above 1000 °C and time over 120 min as shown in Fig. 11. Thus, in terms of the aspect ratio of crystals, it is necessary to hold the glass for a maximum of 120 min in order to produce the highest mechanical properties (K_{1c}, see Table 5).

Fig. 12 presents the XRD patterns of glass-ceramics with increasing heat treatment temperature and the results clearly suggest an increasing crystallinity as the temperature increased, judging from the peak in the range of 20–40°. The crystalline phase appearing in Fig. 12 was not matched in the JCPDS file and was found to be a monoclinic crystal structure having a crystal volume = 246.621 Å^3, with lattice parameters, $a=6.6862$Å, $b=8.3084$Å, $c=4.6477$Å, $\alpha=93.3°$, $\beta=106.4°$, $\gamma=92.9°$ (Table 3). The crystal was rich in TiO_2 and Fe_2O_3 elements compared to the residual glass as shown in Fig. 13 and Table 4 and was found to be $(Ca_{0.05})Al\ Si_{0.75}\ P_{0.5}\ O_{4.5}$ by EDS.

3.3. Properties of the glass-ceramic

The physical and thermal properties of the glass and glass-ceramics are presented in Tables 5 and 6. Observation of crack propagation and interaction with microstructural features indicated that crack deflection occurred more readily in the higher aspect ratio samples (Fig. 14). Based on the previous result of the mechanical properties of K-F-richterite glass-ceramic,[16] it was assumed that the higher aspect ratio of the crystal

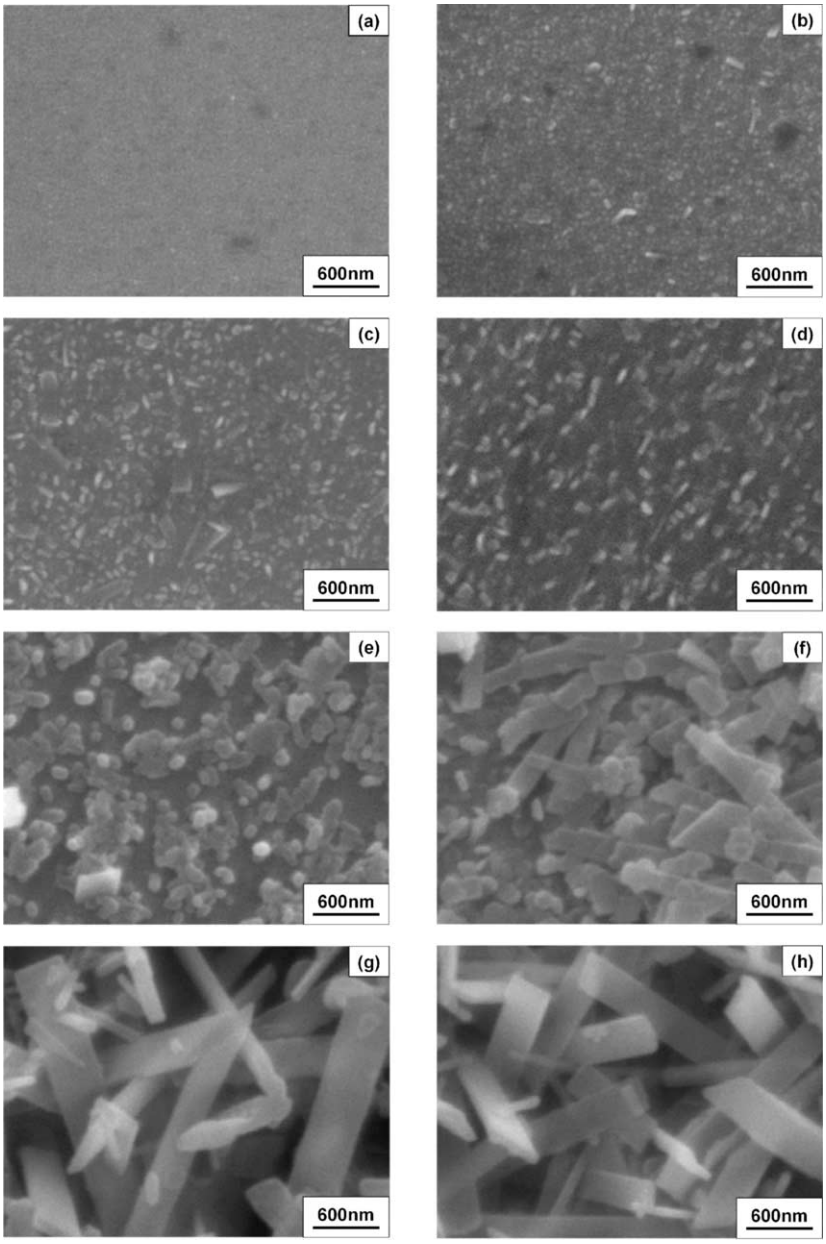

Fig. 7. Sequence of crystal growth with change of time at 950 °C : for (a) 5, (b) 10, (c) 15, (d) 25, (e) 30, (f) 60, (g) 120, (h) 240 min.

would have higher fracture toughness (see Table 5: Fracture toughness as function of heat treatment condition).

Fig. 15 shows the relationship between the hardness, wear resistance and the microstructure (crystallinity, crystal size) with a modified T–T–T (temperature–time–transformation) diagram. Hardness is directly related to strength, elastic constants and crystallinity of glass-ceramics. Thus the relative value of hardness in Fig. 15 suggests the strength and elastic constant are related to temperature and time. With increasing temperature, the heat treatment time for higher crystallinity of glass-

Table 2
Chemical composition of glass and droplets (in wt.%)

Element	Glass (a)	Droplet (b)
O K	25.12	31.67
FeL	7.27	17.85
MgK	0.96	0.99
AlK	11.82	9.59
SiK	34.83	19.20
K K	1.53	0.51
CaK	13.86	7.59
TiK	4.61	12.59
Total	100	100

Table 3
Miller indices and relative intensity of a new crystal diffraction patterns from Fig. 12(c)

Angle (2θ)	d-spacing (Å)	h	k	l	Relative intensity (%)
18.08	4.9007	1	1	0	20.5
19.91	4.4536	0	0	1	51.5
21.94	4.0478	0	−1	1	25.7
23.17	3.8340	−1	−1	1	53.6
23.65	3.7573	−1	1	1	100.0
25.59	3.4779	−1	2	0	57.7
26.46	3.3657	1	2	0	31.3
27.53	3.2373	1	0	1	94.8
27.88	3.1970	2	0	0	65.9
29.68	3.0071	−1	−2	1	67.8
31.15	2.8692	−2	1	1	33.9
31.46	2.8415	−2	−1	1	31.2
32.41	2.7604	0	3	0	36.5
34.17	2.6216	−2	2	0	41.6
34.50	2.5978	−1	3	0	31.6
34.88	2.5704	−1	3	0	44.8
36.64	2.4509	2	2	0	14.1
39.31	2.2901	−1	3	1	16.9
39.70	2.2687	0	3	1	10.4
43.74	2.0677	−1	−2	2	15.8
44.62	2.0292	−2	−3	1	16.9
48.46	1.8771	−2	2	2	15.3
48.95	1.8594	2	−3	1	12.3
53.53	1.7104	−2	−3	2	15.4
55.67	1.6498	1	−3	2	13.2
62.03	1.4949	−4	−1	2	10.0

Table 4
Composition of residual glass and internal crystal (in wt.)

Element	Glass (a)	Internal crystal (b)
O K	25.59	40.42
MgK	0.78	1.19
AlK	12.48	8.52
SiK	32.23	18.26
CaK	13.43	6.65
TiK	9.58	12.97
FeK	5.91	11.99
Total	100	100

ceramics decreased. At 1050 °C, only a short time was needed for glass-ceramics with good mechanical properties, however, at above 1050 °C, the glass-ceramic was deformed after holding for 30 min due to the thermal effect, approaching the lower viscosity region of glass. A similar result was found at 950 °C for 480 min and at 1000 °C for 240 min, which were found to be the critical times and temperatures, after which deformation occurred.

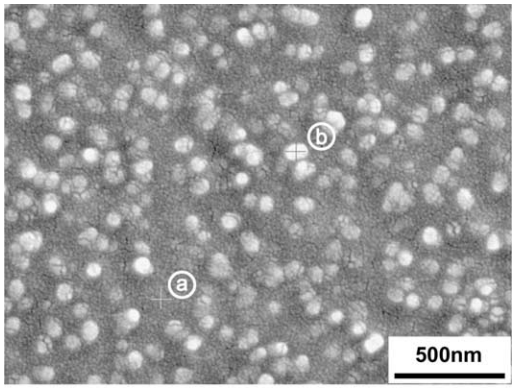

Fig. 8. SEM photograph of the etched polished glass heat treated at 880 °C for 10 min. The regions of cross mark in the photos were analyzed by EDS (Table 2). (a) Glass and (b) droplet.

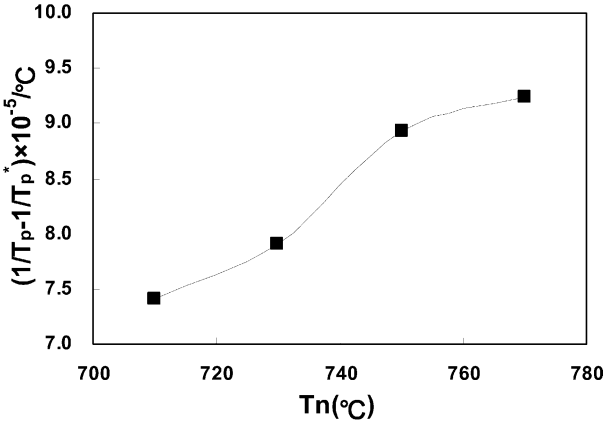

Fig. 9. DTA crystallization temperature ($1/T_p - 1/T_p^o$) for the glass (10 wt.%CaO–5 wt.%TiO_2) as a function of heat treatment temperature (T_n).

Table 5
Density, crystallinity, hardness and crystal phases of glass-ceramics

Condition (°C)	Density (g/cm^3)	Crystallinity (%)[a]	Hardness (GPa)	Fracture toughness (MPa m$^{1/2}$)[a]	Coefficient of thermal expansion ($\times 10^{-6}$/K)
950	2.777	54	7.04	1.121	5.76
1000	2.778	82	7.42	1.681	5.49
1050	2.783	90	7.26	1.860	6.49

[a] Ref. 17.

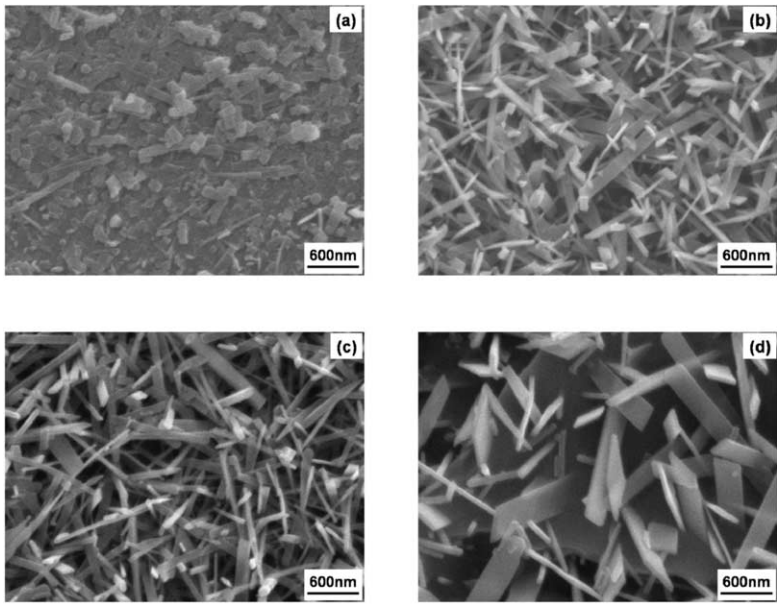

Fig. 10. SEM microstructure (crystal size) of glass-ceramic heat treated at (a) 950 (b) 980 (c) 1000 and (d) 1020 °C for 60 min under one stage heat treatment (simultaneously, nucleation and crystal growth).

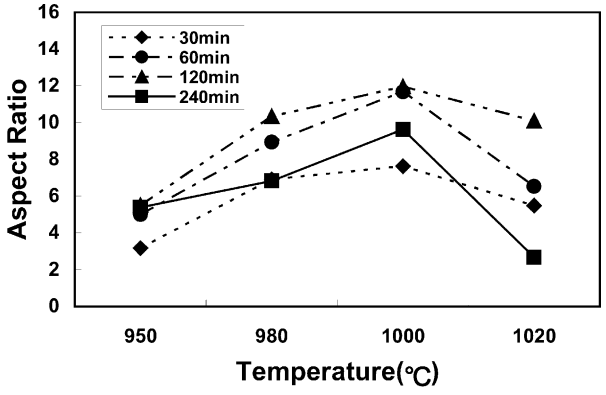

Fig. 11. Aspect ratio of internal crystals as a function of temperature and time.

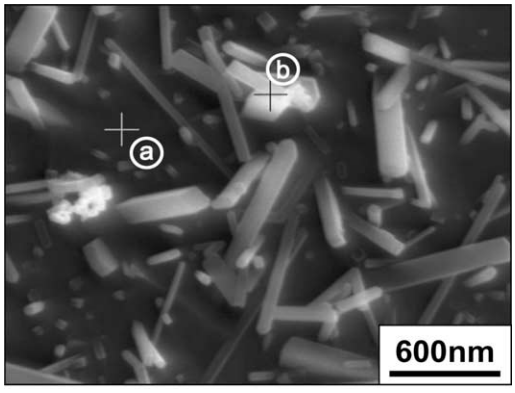

Fig. 13. The region of residual glass and internal crystal of glass-ceramic ($10CaO–7TiO_2$) heat treated at 1000 °C for 60 min for EDS analysis (a) residual glass and (b) crystal.

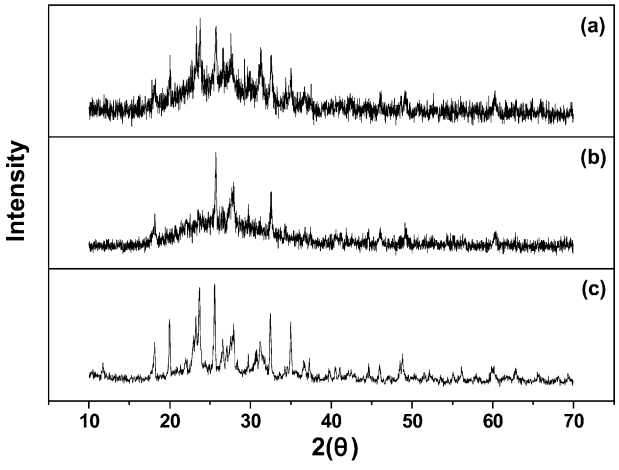

Fig. 12. X-ray powder diffraction patterns of glass-ceramic (CaO–10 wt.%, TiO_2–7 wt.%) heat treated at (a) 950 (b) 1000 and (c) 1050 °C for 60 min.

Table 6
Summary of physical and thermal properties of glass and glass-ceramic

Properties	Glass	Glass-ceramic
Density (g/cm^3)	2.765	2.774–2.806
Hardness (GPa)	6.03	6.20–7.60
Strength (MPa)	82.43	98–176
Elastic constant (GPa)[a]	93	91–100
Fracture toughness (MPa $m^{1/2}$)[a]	0.996	1.121–3.100
Erosion rate (g/cm^2)[a]	7.052×10^{-3}	$5.052–1\times10^{-3}$
Thermal expansion coefficient (/K)	6.02×10^{-6}	$5.49–6.49\times10^{-6}$

[a] Ref. 17.

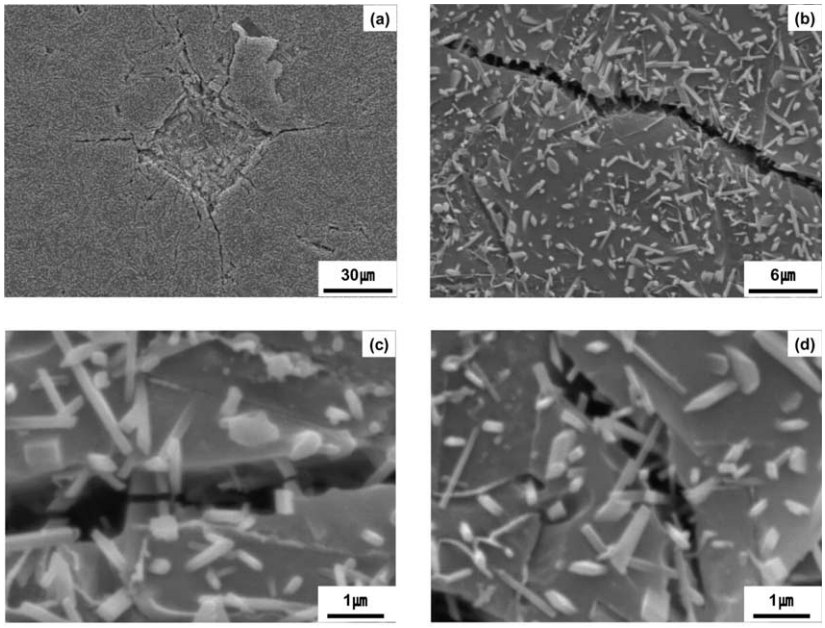

Fig. 14. SEM micrographs showing crack propagation in the glass-ceramic (at 1050 °C for 240min) (etched sample after indenting) (a) indent size and cracks, under 1 kg of Vickers load (b) a whole crack length (c) a part of cracks near the indent and (d) the end of cracks far from the indent.

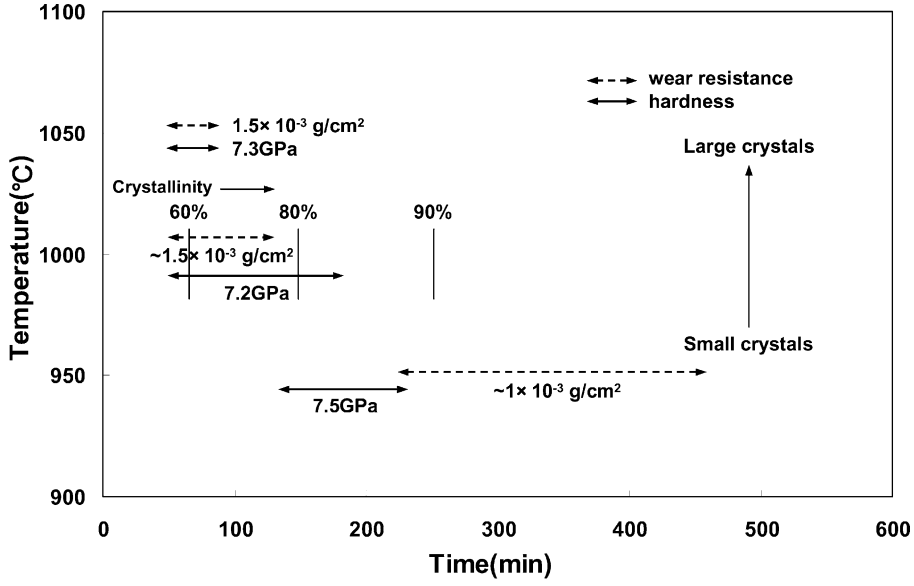

Fig. 15. Optimum heat treatment condition for producing a glass-ceramic using fly ash produced from a power plant in terms of physical properties of materials.

4. Conclusion

Vitrification of coal fly ash was found to be difficult, and crystallization of the molten glass was not possible without modifying the composition of the fly ash. With cheap material as a source of CaO, shell was added into the fly ash at a low melting temperature and a small amount of TiO_2 was used as a nucleating agent. Under a single stage heat treatment, a crystalline phase formed in the microstructure of glass-ceramics with a crystal size of $2.09\times0.36\times0.096$ μm^3 and a high aspect ratio. Glass-ceramics produced at an optimum heat treatment condition showed sufficiently high wear resistance and fracture toughness to be used in building materials requiring good mechanical properties.

References

1. Mukherji, S. K., Machhoya, B. B., Savsani, R. M., Vyas, D. R. and Dan, T. K., The utilisation of fly ash in the preparation of ceramic tableware and artware. *Br. Ceram. Trans.*, 1993, **92**(6), 254–257.
2. Iyer, R. S. and Scott, J. A., Power station fly ash. *Resources, Conservation and Recycling*, 2001, **31**, 217–228.

3. Duan, R. G., Liang, K. M. and Gu, S. R., Effect of changing TiO_2 content on structure and crystallization of CaO–Al_2O_3–SiO_2 system glasses. *J. Eur. Ceram. Soc.*, 1998, **18**, 1729–1735.
4. Khater, G. A., The use of Saudi slag for the production of glass-ceramic materials. *Ceramic International*, 2002, **28**, 59–67.
5. Leroy, C., Ferro, M. C., Monteiro, R. C. C. and Fernandes, M. H. V., Production of glass-ceramics from coal ashes. *J. Eur. Ceram. Soc.*, 2001, **21**, 195–202.
6. Barbieri, L., Ferrari, A. M., Lancellotti, I. and Leonelli, C., Crystallization of (Na_2O–MgO)–CaO–Al_2O_3–SiO_2 glassy systems formulated from waste products. *J. Am. Ceram. Soc.*, 2000, **83**(10), 2515–2520.
7. Cioffi, R., Pernice, P., Aronne, A., Catauro, M. and Quattroni, G., Glass-ceramic from fly ash added MgO and TiO_2. *J. Eur. Ceram. Soc.*, 1994, **14**, 517–521.
8. Barbieri, L., Lancellotti, I., Manfredini, T., Queralt, I., Rincon, J. M. and Romero, M., Design, obtainment and properties of glasses and glass-ceramics from coal fly ash. *Fuel*, 1999, **78**, 271–276.
9. Boccaccini, A. R., Buecker, M., Boessert, J. and Marszalk, K., Glass matrix composites from coal ash and waste glass. *Waste Manage*, 1997, **17**, 39–45.
10. Rabinovich, E. M., Glass-ceramics from Israeli slag and coal ash. In *Nucleation and Crystallisation in Glasess*, ed. J. S. Simmons, D. R. Hulmann and G. H. Beall. American Ceramic Society, New York, 1982, pp. 334–340.
11. Sheng, J., Huang, B. X., Zhang, J., Zhang, H., Sheng, J., Yu, S. and Zhang, M., Production of glass from coal fly ash. *Fuel*, 2003, **82**, 181–185.
12. Erol, M., Demirler, U., Küçükbayrak, S., Ersoy-Meriçboyu, A. and Öveçoğlu, M. L., Characterization investigations of glass-ceramics developed from Seyitömer thermal power plant fly ash. *J. Eur. Ceram. Soc.*, 2003, **23**, 757–763.
13. Anstis, G. R., Chantikul, P., Lawn, B. R. and Marshall, D. B., A critical evaluation of indentation techniques for measuring fracture toughness, direct measurements. *J. Am. Ceram. Soc.*, 1981, **64**, 533–538.
14. Lee, S. W., Deshpande, V., Stevens, R. and Knott, P., Determination of the nucleation rate curve for lead titanate glass by differential thermal analysis. *Phys. Chem. Glasses*, 1996, **37**(6), 223–226.
15. Tammann, G., *The States of Aggregation*. D. Van Nostrand Co, NY, 1925.
16. Beall, G. H., Design and properties of glass-ceramics. *Annu. Rev. Mater. Sci.*, 1992, **22**, 91–119.
17. Kim, J. M. and Kim, H. S., Development and physical properties of a glass-ceramic from fly ash of power station. *J. Kor. Ceram. Soc.*, 2002, **39**(6), 558–565.